results. The smaller the downhill barrier, the closer we expect r_f to be to unity, and hence the shorter the downhill path length, i.e., the geometrical distortion from the corresponding minimum. Recent applications of this principle extend to enzyme catalysis and protein engineering. For example, correlation between the transition state structure and destabilization of the native state of chymotrypsin inhibitor 2 by mutation suggests that unfolding proceeds by way of an ensemble of related transition states (*24*). Using the present results in a more quantitative fashion, perhaps in combination with models such as Marcus theory (*25*), is a likely area of future research.

One aspect of the complex phenomenology of glasses is the appearance of anomalous heat capacities and conductivities at low temperature. It has been suggested that these properties are due to quantum tunneling between pairs of minima referred to as two-level systems (TLSs) (*26–28*). Angell (*29*) has further associated TLSs with the low-frequency excess vibrational density of states observed in many glasses, known as the "boson peak." For tunneling between two minima to be significant, they must be separated by a low, narrow barrier, which suggests that the present theory may apply. Results are shown in Fig. 3 for more than 10^4 pathways calculated for several bulk model atomic glass-formers, as described in detail elsewhere (*30*). This database contains a number of very short paths, and we see that these do indeed have $r_f \approx 1$. The asymmetric "staircase" profile now established for long-range interactions above is expected to produce more efficient local relaxation to low-energy structures. However, this observation in itself is not sufficient to predict the glass-forming propensity, which depends on longer-ranged correlations between features of the PES.

High-resolution spectroscopy has recently provided detailed insight into the dynamics of weakly bound complexes, particularly water clusters (*31*), and has inspired much theoretical work. The present theory is equally applicable to small molecules, and results are presented in Fig. 4 for pathways between the "crown" and global minimum geometries of $(H_2O)_3$, calculated ab initio with various different basis sets and treatments of the correlation energy. Again, we see that r_f is close to unity for the low-barrier side of the path, and the ratio is generally nearer to its ideal value for the shortest path lengths. It may be possible to exploit such results in quantum dynamics calculations and analysis of intermolecular forces.

Correlations between structure, dynamics, and thermodynamics are important throughout molecular science. The present results provide new tools to tackle such problems, with a wide range of possible applications.

References and Notes

1. P. E. Leopold, M. Montal, J. N. Onuchic, *Proc. Natl. Acad. Sci. U.S.A.* **89**, 8721 (1992).
2. J. D. Bryngelson, J. N. Onuchic, N. D. Socci, P. G. Wolynes, *Proteins* **21**, 167 (1995).
3. P. G. Wolynes, J. N. Onuchic, D. Thirumalai, *J. Chem. Phys.* **102**, 1619 (1995).
4. C. A. Angell, *Science* **267**, 1924 (1995).
5. F. H. Stillinger, *Science* **267**, 1935 (1995).
6. J. P. K. Doye, D. J. Wales, *J. Chem. Phys.* **105**, 8428 (1996).
7. K. D. Ball, R. S. Berry, R. E. Kunz, F. Y. Li, A. Proykova, D. J. Wales, *Science* **271**, 963 (1996).
8. N. D. Socci, J. N. Onuchic, P. G. Wolynes, *Proteins Struct. Funct. Genet.* **32**, 136 (1998).
9. P. G. Mezey, *Potential Energy Hypersurfaces* (Elsevier, Amsterdam, 1987).
10. R. Thom, *Stabilité Structurelle et Morphogénèse* (Benjamin, New York, 1972).
11. R. Gilmore, *Catastrophe Theory for Scientists and Engineers* (Wiley, New York, 1981).
12. Stationary points of molecular systems possess zero eigenvalues when the energy is invariant with respect to overall translation or rotation.
13. P. M. Morse, *Phys. Rev.* **34**, 57 (1929).
14. P. A. Braier, R. S. Berry, D. J. Wales, *J. Chem. Phys.* **93**, 8745 (1990).
15. J. P. K. Doye, D. J. Wales, *J. Chem. Soc. Faraday Trans.* **93**, 4233 (1997).
16. M. A. Miller, J. P. K. Doye, D. J. Wales, *J. Chem. Phys.* **110**, 328 (1999).
17. ———, *Phys. Rev. E* **60**, 3701 (1999).
18. More details are given in the supplementary material available on *Science* Online at www.sciencemag.org/cgi/content/full/293/5537/2067/DC1.
19. J. P. K. Doye, D. J. Wales, *J. Phys. B* **29**, 4859 (1996).
20. ———, *Science* **271**, 484 (1996).
21. R. S. Berry, N. Elmaci, J. P. Rose, B. Vekhter, *Proc. Natl Acad. Sci. U.S.A.* **94**, 9520 (1997).
22. D. J. Wales, J. P. K. Doye, M. A. Miller, P. N. Mortenson, T. R. Walsh, *Adv. Chem. Phys.* **115**, 1 (2000).
23. G. S. Hammond, *J. Am. Chem. Soc.* **77**, 334 (1955).
24. A. Fersht, *Structure and Mechanism in Protein Science* (Freeman, New York, 1999).
25. R. A. Marcus, *Annu. Rev. Phys. Chem.* **15**, 155 (1964).
26. P. Anderson, B. Halperin, C. Varma, *Philos. Mag.* **25**, 1 (1972).
27. W. Phillips, *J. Low Temp. Phys.* **7**, 351 (1972).
28. R. Zeller, R. Pohl, *Phys. Rev. B* **4**, 2029 (1971).
29. C. A. Angell, *J. Phys. Condens. Matter* **12**, 6463 (2000).
30. T. F. Middleton, D. J. Wales, *Phys. Rev. B* **64**, 024205 (2001).
31. K. Liu, J. D. Cruzan, R. J. Saykally, *Science* **271**, 929 (1996).
32. F. H. Stillinger, T. A. Weber, *Phys. Rev. B* **31**, 5262 (1985).
33. S. Sastry, P. G. Debenedetti, F. H. Stillinger, *Nature* **393**, 554 (1998).

34. This paper is dedicated to R. S. Berry on the occasion of his 70th birthday. I am grateful to J. Kobine for discussions concerning catastrophe theory, and to J. Doye and A. Kirby for helpful comments.

16 May 2001; accepted 2 August 2001

Active Normal Faulting in the Upper Rhine Graben and Paleoseismic Identification of the 1356 Basel Earthquake

Mustapha Meghraoui,[1]* Bertrand Delouis,[2] Matthieu Ferry,[2] Domenico Giardini,[2] Peter Huggenberger,[3] Ina Spottke,[3] Michel Granet[1]

We have identified an active normal fault in the epicentral area of the Basel (Switzerland) earthquake of 18 October 1356, the largest historical seismic event in central Europe. The event of 1356 and two prehistoric events have been characterized on the fault with geomorphological analysis, geophysical prospecting, and trenching. Carbon-14 dating indicates that the youngest event occurred in the interval 610 to 1475 A.D. and may correspond to the 1356 Basel earthquake. The occurrence of the three earthquakes induced a total of 1.8 meters of vertical displacement in the past 8500 years for a mean uplift rate of 0.21 millimeters per year. These successive ruptures on the normal fault indicate the potential for strong ground movements in the Basel region and should be taken into account to refine the seismic hazard estimates along the Rhine graben.

To understand the damage produced by past earthquakes and to forecast future earthquake scenarios, an analysis of potentially active faults and related seismogenic behavior is required. An earthquake on 18 October 1356 destroyed the city of Basel, Switzerland, and damaged large parts of the upper Rhine graben (Fig. 1). This large earthquake had an epicentral intensity of IX to X on the MSK scale (*1*) and an estimated magnitude of 6.0 to 6.5 (*2*, *3*). Thirty to 40 castles were destroyed within a 10-km radius around Basel, and castles, towers, and churches within a 200-km radius were damaged (*2*, *3*) (Fig. 2). The Basel region belongs to an area with a low seismicity level and a long seismic cycle. Basic knowledge on seismogenic faults in this area is lacking, and the hazards evaluation depends on the sporadic occurrence of large earthquakes. To determine the activity and recurrence rate of earthquakes near Basel, we need, first, to identify the fault

along which the 1356 earthquake occurred and, second, to reconstruct its seismogenic history.

The Basel region belongs to the upper Rhine graben and its related Cenozoic rift system, which is limited to the south by the fold-and-thrust belt of the Jura Mountains. The background seismicity of the graben is relatively modest in comparison with that of other continental rifts. Regional studies with local seismic networks show a more pronounced seismicity to the east and south of the graben; the seismogenic layer has a depth of about 15 km within the graben, reaching 20-km depth beneath the Black Forest and Swiss Jura Mountains (*4*). Until now, the nature of the 1356 earthquake has remained an open question, and several authors have discussed the possible seismogenic structures in the area (*5*). Focal mechanisms calculated for several tens of earthquakes with Richter magnitude (M_L) $\leq$ 5 in the region of the southern upper Rhine graben and northern Alpine foreland show the predominance of normal faulting and strike slip with ENE-WSW direction of extension (*6*).

We identified the NNE-SSW–trending Basel-Reinach escarpment, which is 8 km long and 30 to 50 m high, as the surface expression of an active fault (Fig. 3). Oligocene sandstones with intercalated clay layers dipping 10° west constitute the pre-Quaternary substratum that crops out along the scarp. The substratum is overlain by a succession of alluvial terraces, and the uppermost terrace is attributed to the middle Pleistocene (*7*). At depth, seismic profiles across the fault scarp show about 100 m of vertical offset at 600-m depth, which may correspond to the lower Oligocene (Web fig. 1) (*8*). At the surface, the linear morphology of the scarp also indicates the active character of the fault. Younger terraces attributed to the Pleistocene, which likely belong to the old meanders of the Birs River, are uplifted along the scarp (Fig. 3).

The examination of aerial photos shows late Pleistocene and Holocene deposits that constitute alluvial terraces as well as young alluvial fans visible along the scarp toe. Although the fault is not directly visible, its presence can be inferred from the exposed old meanders and steplike morphology along the scarp that suggest its progressive uplift during the late Quaternary. Furthermore, the drainage pattern visible on the footwall block is characterized by short and deep stream incisions along tributary creeks to the east and long meandering streams to the west, which illustrate a morphological asymmetry typical of an active normal fault (Fig. 3). The fault-controlled escarpment is visible immediately south of the city of Basel, but it is partly hidden by the suburban settlements, agricultural fields, and small forests. The fault zone is located between the steep slope of the scarp and the flat fields of the Birs Valley. To locate the fault more precisely for trenching, we carried out electrical resistivity, ground-penetrating radar, and seismic reflection profiles across the scarp and the adjacent young alluvial fan.

We dug several trenches at each of two sites (Fig. 3). The three trenches at site 1 were not longer than 10 m because of trees, but they displayed faulted young deposits. Four parallel trenches (T1 to T4) at site 2 crossed 75 m of the scarp; trenches T1 and T3 were about 70 m long each, and trenches T2 and

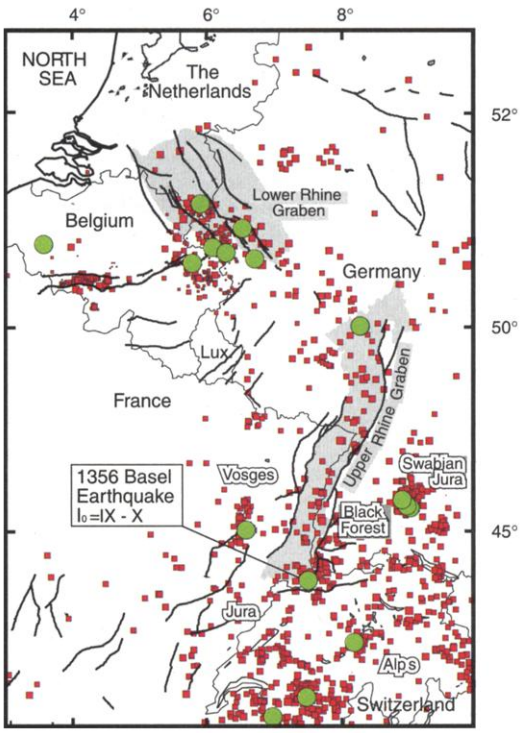

Fig. 1. Seismotectonic framework of the central European region around Basel (*14*). Grabens are limited by Quaternary faults. Squares depict the instrumental seismicity from 1910 to 1990 ($1 < M < 5.5$). Circles correspond to the historical seismicity since 1350 ($M > 5.0$).

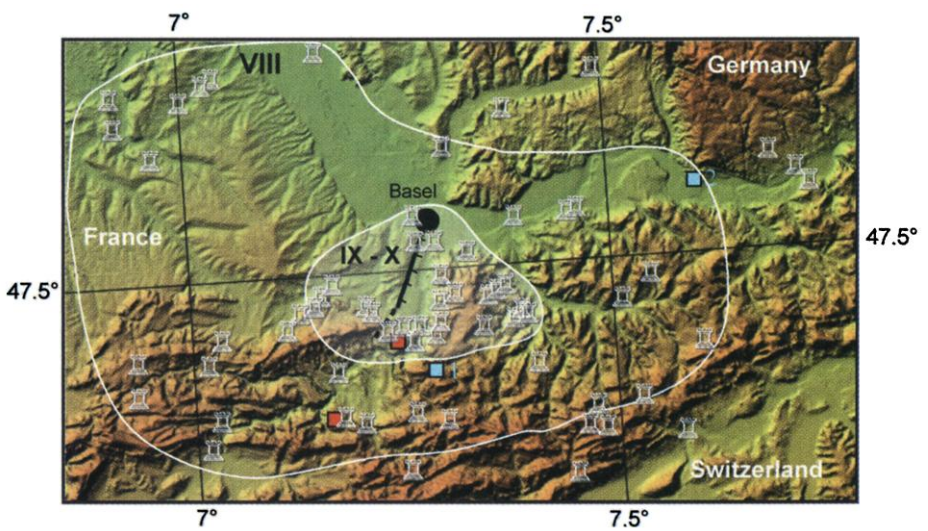

Fig. 2. Isoseismals VIII and IX to X of the 1356 Basel earthquake and the locations of damaged medieval castles (*2*, *3*). The active fault (solid black line) is in the Birs Valley, south of Basel. Note also the locations of caves (red squares) and Berg and Seewen lakes (blue squares) in the area (*12*). The magnitude of the Basel earthquake and spatial distribution of the damage suggest a shallow focal depth and a fault length of 10 to 15 km; events of this size are generally expected to induce coseismic surface deformation.

[1]Ecole et Observatoire des Sciences de la Terre–Institut de Physique de Globe (EOST-IPAS), 5 rue René Descartes, 67084 Strasbourg, France. [2]Institut of Geophysics, Department of Seismology and Geodynamics, Eidgenössische Technische Hochschule, Hoenggerberg, CH-8093, Zurich, Switzerland. [3]Geologisch-Paläontologisches Institut, Universität Basel, Bernoullistrasse 16, CH-4056, Switzerland.

*To whom correspondence should be addressed. E-mail: mustapha@eost.u-strasbg.fr

T4, each about 20 m in length, were dug to constrain observations of faulted late Quaternary units. Evidence of normal faulting and surface deformation was found in all of the trenches, confirming the geomorphological and geophysical observations (Web fig. 1 and Fig. 4). At site 2, the main fault consists of two branches with minor antithetic faulting and warped units (*9*).

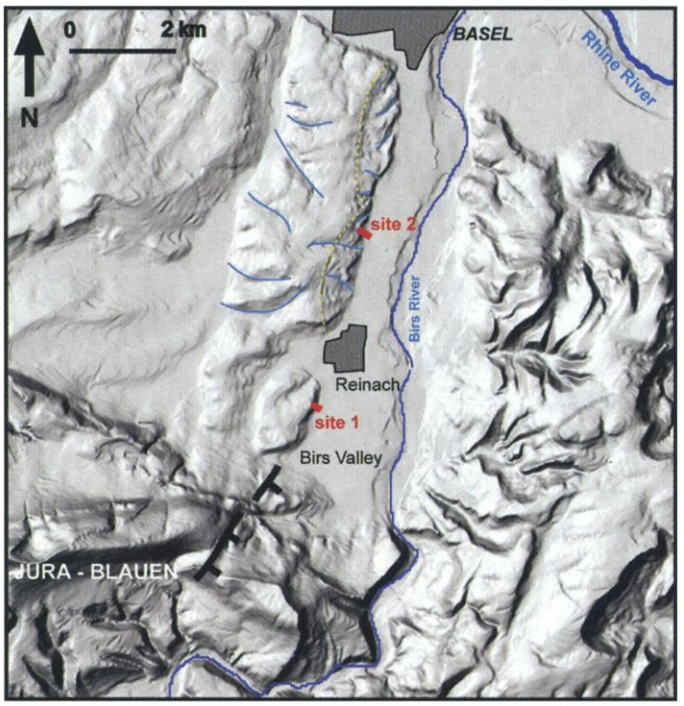

Fig. 3. Geomorphology of the Birs Valley and the Basel-Reinach fault scarp from a high-resolution topography (MNT25, Office fédéral de topographie, DV1441) and paleoseismic sites 1 and 2. Rivers are shown by blue lines. Note the uplifted Birs River terraces (yellow lines) on the footwall along the northern strand of the fault and the southern fault continuation (black dashed line) across the Jura.

Trench T4 intercepted a fault that displaces young colluvial wedge deposits (Fig. 4A). This fault branch is located at the base of the steep slope of the scarp. The successive fault scarp degradation and related unconformities record the cumulative vertical movements associated with past earthquakes (Fig. 4B). The uppermost unit A below the present soil corresponds to a 0.5-m-thick colluvial wedge deposit consisting of mixed gravels and silty-clay layers that postdate the most recent fault displacement (Fig. 4C). Carbon-14 dating of a bulk soil sample collected at the base of unit A gives an age of 460 ± 25 years B.P., which yields a calibrated 2σ date of 1410 to 1475 A.D. (*10*). Unit B also consists of a 0.5-m-thick colluvial wedge deposit with coarse gravels and silty-clay units at the base of which ^{14}C dating of a bulk soil sample gives 1310 ± 70 years B.P. (2σ date = 610 to 890 A.D.). Unit C is a 0.8-m-thick colluvial deposits comparable to units A and B but with nearly flat lying units of coarse and fine gravels, abruptly cut by the fault. The ^{14}C dating of a bulk soil sample of unit C yields an age of 2430 ± 120 years B.P. (2σ date = 850 to 200 B.C.). A succession of massive colluvial

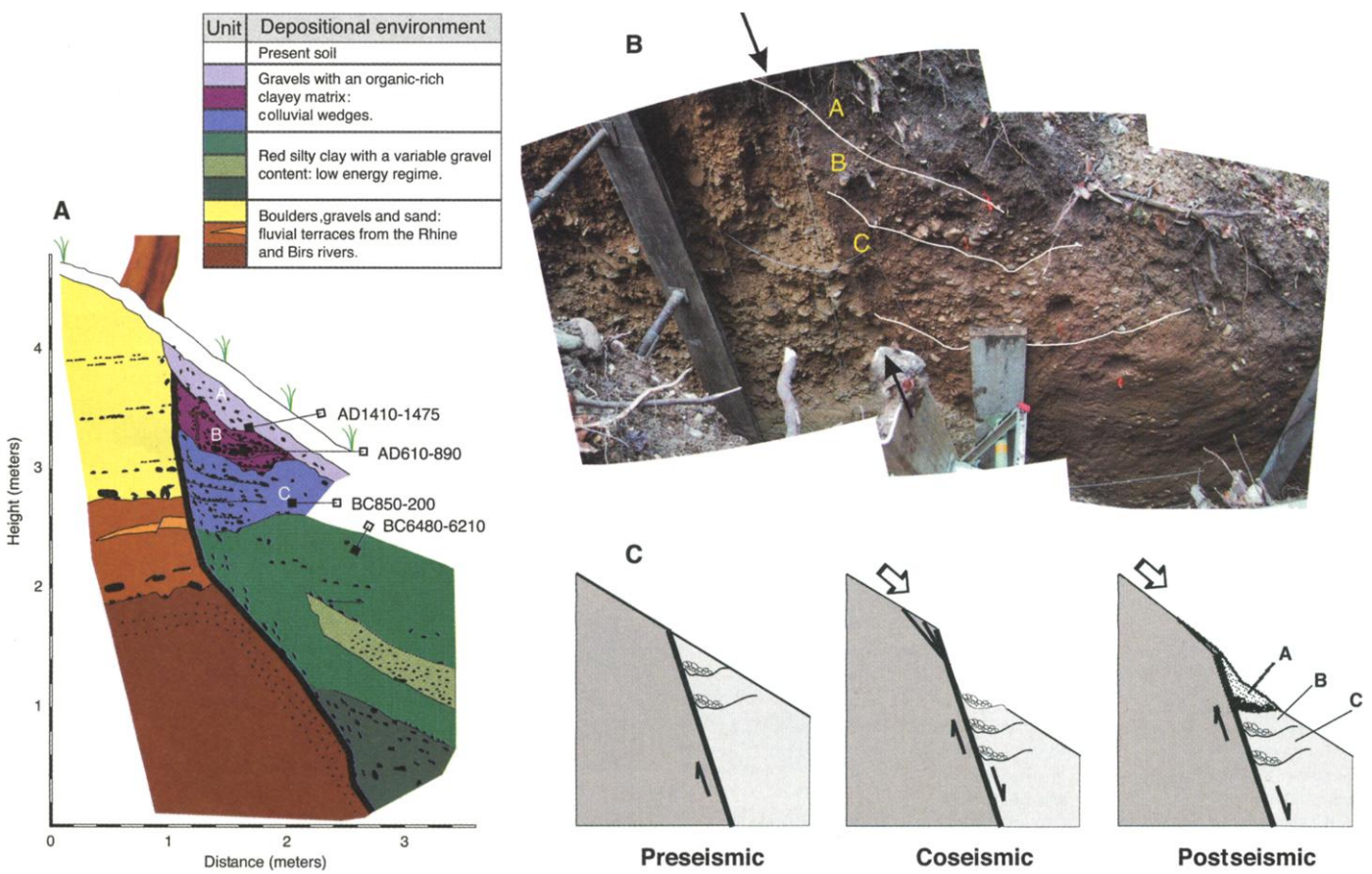

Fig. 4. (**A**) Trench T4 north wall illustrating the surface faulting with the three most recent displacements and colluvial wedge deposit A that postdate the 1356 earthquake. (**B**) Photomosaic of colluvial wedges A, B, and C. (**C**) Reconstruction of paleoseismic events: The fault scarp degradation and related colluvial wedge deposit A record the most recent earthquake.

silt layers with scattered gravels is observed below unit C, and the ^{14}C dating of a bulk soil sample of the uppermost layers yields 7510 ± 80 years B.P. (2σ date = 6480 to 6210 B.C.). The succession of faulted colluvial wedges B and C overlain by unit A indicates three seismic ruptures with at least 1.8 m of cumulative vertical displacements (corresponding to the thickness of the three colluvial wedges A, B, and C of Fig. 4B) during the past 8500 years. The most recent faulting event is bracketed between 610 and 1475 A.D. It occurred before the deposition of unit A (before 1410 to 1475 A.D.), and it may correspond to the 1356 A.D. Basel earthquake.

The 0.5 to 0.8 m of vertical displacements measured in trench T4 is consistent with large earthquakes that rupture through the entire seismogenic thickness (15 km) over a length of 15 to 20 km (*11*). These fault dimensions would yield an estimated seismic moment M_o = 3 to 5 10^{25} dyne cm (moment magnitude M_w = 6.4 to 6.5) in good agreement with the historical estimates (*2*, *3*). However, only an 8-km-long Basel-Reinach fault is visible in the Birs Valley; the fault zone may extend to the north (below the city area) and to the south across the Jura Mountains.

In addition to the 1356 earthquake, measurements from the trenches identify two other events that occurred between 6480 to 850 B.C. and 850 B.C to 890 A.D. These results are consistent with (i) the analysis of growth anomalies in speleothems in caves and (ii) deformed layers in lake deposits south of the Birs Valley (Fig. 3) (*12*). A consistent pattern appears from these different investigations and points to a recurrence time for a 1356-type earthquake in the Basel area of about 1500 to 2500 years. The occurrence of three large earthquakes in the past 8500 years on the Basel-Rheinach fault yields a mean uplift rate of 0.21 mm/year and is compatible with geodetic and seismic estimates of uplift rate farther north in the Rhine graben (*13*). We conclude that the Basel-Reinach fault accommodates the major part of the seismic activity of the area. A frequency-magnitude distribution of the seismicity during the past 1000 years has been determined for the seismic hazard assessment in the greater Basel region (Fig. 5). Assuming stationary seismicity, the 1000-year activity rate can be extrapolated for a 10,000-year period by scaling the curve by one logarithmic unit, inferring 20 1356-type earthquakes (curve A, Fig. 5). Combining paleoseismic results along the Basel-Reinach fault, we obtain instead five to eight 1356-type earthquakes for the last 10,000 years and a more constrained distribution for the occurrence rate of earthquakes in the Basel region (curve B, Fig. 5).

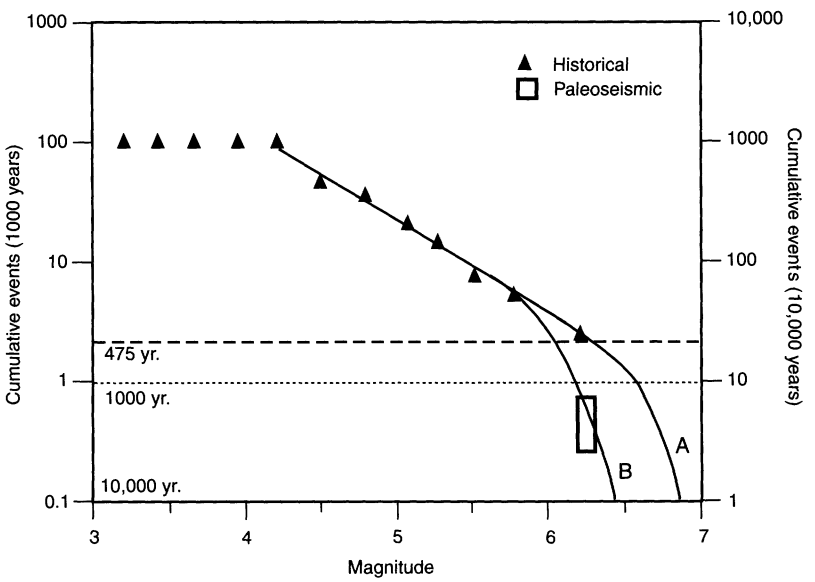

Fig. 5. Cumulative logarithmic frequency-magnitude distribution of the seismicity of the past 1000 years in the greater Basel region, from the Macroseismic Earthquake Catalogue of Switzerland. The activity rates constrained by the historical and paleoseismological records are similar at low magnitudes but very different at higher magnitudes. The difference is also modest for the 475-year return period commonly assumed in hazard mapping but becomes dominant for longer return periods and low occurrence probabilities.

References and Notes

1. Medvedev-Sponhauer-Karnik (MSK) intensity scale or modified Mercalli scale; see also V. Karnik [*Seismicity in the European Area*, part I (Reidel, Dordrecht, Netherlands, 1969)]. Mayer-Rosa and Cadiot (*2*) assigned an MSK intensity of IX to X for the main shock and determined an epicentral location in the Birs Valley a few km south of Basel.
2. D. Mayer-Rosa, B. Cadiot, *Tectonophysics* **53**, 325 (1979).
3. B. Cadiot *et al.*, in *Les Tremblements de Terre en France*, J. Vogt, Ed., *Mem. Bur. Recherche Géol. Minières* **96**, 154 (1979). Several contemporary reports (including Jean de Roquetaillade, 1360; K. von Waltenkof, 1360; F. Closener, 1362; P. Despotots, 14th to 15th century; Petrarca, 14th century) describe the aftershock activity and several seismic events on the 18 October 1356, with a first strong shock in the evening "at the dinner time" (7 to 8 p.m.) and a second stronger main shock "at the bed time" (10 p.m.). A 1362 manuscript related to the biography of Pope Innocenzo VI reports ground ruptures associated with the 1356 earthquake.
4. K. P. Bonjer, *Tectonophysics* **275**, 41 (1997).
5. B. Meyer *et al.* [*Terra Nova* **6**, 54 (1994)] infer that the Basel earthquake may have reactivated a basement thrust fault beneath the shallow-depth aseismic detachment that underlies the Jura Mountains; B. Nivière and T. Winter [*Global Planet. Change* **27**, 263 (2000)] question the role of thrusting as a seismogenic source, and J. H. Illies and G. Greiner [*Geol. Soc. Am. Bull.* **89**, 770 (1978)] and J. P. Brun *et al.* [*Geology* **19**, 758 (1991)] correlate the seismic activity with normal faulting imaged by reflection seismic lines across the graben.
6. B. Delouis *et al.*, *Tectonophysics* **221**, 413 (1993); T. Plenefisch, K. P. Bonjer, *Tectonophysics* **275**, 71 (1997).
7. P. Bitterli-Brunner, H. Fischer, Atlas géologique de la Suisse, 1067 Arlesheim (1/25000) (Commission Géologique Suisse, Kummerly and Frey S.A., Editions géographiques, Berne, Switzerland, 1988).
8. Web fig. 1 is available on *Science* Online at www.sciencemag.org/cgi/content/full/293/5537/2070/DC1.
9. Evidence of late Quaternary faulting was recognized in trenches (see also Fig. 4): (i) a 10-cm-thick zone of sheared sedimentary deposits with warped footwall units and faulted silty layers on the hanging wall, (ii) alternating layers of sandy to silty deposits with coarse-grained gravels on the hanging wall and successive organic-rich colluvial wedge deposits, (iii) colluvial wedges corresponding to deposits directly associated with the fault scarp degradation immediately after a seismic event (Fig. 4C), and (iv) faulted colluvial wedge deposits with cumulative vertical displacements and secondary ruptures, as well as progressively tilted gravels and sandy-silt units.
10. The radiocarbon date is given in years B.P. (before 1950 or "present"), and the standard deviation is calculated from the laboratory error (count rate statistics). The calendar age is given in B.C. or A.D., and the standard deviation (2σ) is obtained from the radiocarbon date intercept with the calibration curve; see also M. Stuiver *et al.*, *Radiocarbon* **40**, 1041 (1998); C. Bronk-Ramsey, *Radiocarbon* **40**, 461 (1998).
11. H. Kanamori, D. L. Anderson, *Bull. Seismol. Soc. Am.* **65**, 1073 (1975); C. Wells, K. Coppersmith, *Bull. Seismol. Soc. Am.* **84**, 974 (1994).
12. F. Lemeille *et al.* [*Geodyn. Acta* **12**, 179 (1999)] indicate the occurrence of three growth anomalies of speleothems and collapsed rocks in caves dated at 3630 to 3370 B.C., 160 B.C. to 80 A.D., and 1165 to 1400 A.D. A. Becker *et al.* (in preparation) investigated lake deposits in the Berg and Seewen lakes and show the occurrence of possible seismic events between 180 and 1160 B.C., 2900 and 3850 B.C., 4870 and 5660 B.C., 8260 and 940 B.C., and 10,720 and 11,200 B.C.
13. L. Ahorner, *Tectonophysics* **29**, 233 (1975); M. Meghraoui *et al.*, *J. Geophys. Res.* **105**, 13809 (2000); J. M. Nocquet *et al.*, *J. Geophys. Res.* **106**, 11239 (2001).
14. T. Camelbeeck, M. Meghraoui, *Geophys. J. Int.* **132**, 347 (1998).

15. We thank M. Cara, D. Mayer-Rosa, J. Vogt, K. Bonjer, A. Crone, R. Arrowsmith, B. Meyer, E. Jacques, T. Winter, G. Sagripanti, P. Ziegler, and D. Faeh for fruitful discussions; P. Grootes for the detailed reports on ^{14}C dating; W. Lowrie for editorial help; S. Sellami for figure preparation; and the Reinach local authorities for their assistance in the field. This research is funded by Institut National des Sciences de l'Univers–France (99PNRN 20 AS) and Bureau de Recherche Geologique et Minière (GeoFrance 3D 99/17), the project PALEOSEIS (Swiss National Fond and Swiss Commission for the Safety of Nuclear Installations), and the EU project SAFE (EVG1-2000-22005). This research is conducted under the framework of European Correlation (EUCOR)–Upper Rhine Graben Evolution and Neotectonics (URGENT), European Science Foundation Network number 85. This is publication 01012 of EOST-IPGS and 1192 of the Institute of Geophysics, Eidgenössische Technische Hochschule Zurich.

23 April 2001; accepted 29 June 2001